# Induced seismicity associated with fluid injection into a deep well in Youngstown, Ohio

Won-Young Kim [1]

Received 1 February 2013; revised 6 June 2013; accepted 10 June 2013; published 19 July 2013.

[1] Over 109 small earthquakes ($M_w$ 0.4–3.9) were detected during January 2011 to February 2012 in the Youngstown, Ohio area, where there were no known earthquakes in the past. These shocks were close to a deep fluid injection well. The 14 month seismicity included six felt earthquakes and culminated with a $M_w$ 3.9 shock on 31 December 2011. Among the 109 shocks, 12 events greater than $M_w$ 1.8 were detected by regional network and accurately relocated, whereas 97 small earthquakes ($0.4 < M_w < 1.8$) were detected by the waveform correlation detector. Accurately located earthquakes were along a subsurface fault trending ENE-WSW—consistent with the focal mechanism of the main shock and occurred at depths 3.5–4.0 km in the Precambrian basement. We conclude that the recent earthquakes in Youngstown, Ohio were induced by the fluid injection at a deep injection well due to increased pore pressure along the preexisting subsurface faults located close to the wellbore. We found that the seismicity initiated at the eastern end of the subsurface fault—close to the injection point, and migrated toward the west—away from the wellbore, indicating that the expanding high fluid pressure front increased the pore pressure along its path and progressively triggered the earthquakes. We observe that several periods of quiescence of seismicity follow the minima in injection volumes and pressure, which may indicate that the earthquakes were directly caused by the pressure buildup and stopped when pressure dropped.

**Citation:** Kim, W.-Y. (2013), Induced seismicity associated with fluid injection into a deep well in Youngstown, Ohio, *J. Geophys. Res. Solid Earth*, *118*, 3506–3518, doi:10.1002/jgrb.50247.

## 1. Introduction

[2] Since the early 1960s, it has been known that waste disposal by fluid injection at high pressure into subsurface rock formations can cause earthquakes known as induced seismicity [e.g., *Nicholson and Wesson*, 1992; *McGarr et al*., 2002]. There are well-documented cases of induced seismicity including Rocky Mountain Arsenal (RMA), Colorado, in the 1960s [*Healy et al*., 1968]; Ashtabula, Ohio, in the 1980s [*Seeber et al*., 2004]; Paradox Valley, Colorado, in the 1990s [*Ake et al*., 2005]; and Guy, Arkansas, during 2011 [*Horton*, 2012], among others. The largest events at those induced seismicities range from $M_w$ 3.9 at Ashtabula, Ohio, $M_w$ 4.3 at Paradox Valley, $M_w$ 4.7 at Guy, Arkansas, and $M_w$ 4.85 at Rocky Mountain Arsenal [*Herrmann et al*., 1981].

[3] Since early 2011, many significant earthquakes suspected to be induced events occurred in the United States midcontinent region [*Ellsworth et al*., 2012]. They are $M_w$ 5.7 earthquake on 06 November 2011 at Prague, Oklahoma [*Keranen et al*., 2013]; $M_w$ 5.3 event on 23 August 2011 at Trinidad, Colorado [*Rubinstein et al*., 2012; *Viegas et al*., 2012]; $M_w$ 4.8 event on 20 October 2011 at Fashing, Texas [*Brunt et al*., 2012]; $M_w$ 4.8 earthquake on 17 May 2012 at Timpson, Texas [*Brown et al*., 2012]; $M_w$ 4.3 earthquake on 11 September 2011 at Cogdell oil field, Snyder, Texas [*Davis and Pennington*, 1989]; and $M_w$ 3.3 event on 16 May 2009 at Dallas-Fort Worth, Texas [*Frohlich et al*., 2011], and are listed in Table 1. These are broadly related to fluid injection into subsurface strata through disposal wells such as; for secondary recovery of oil (Cogdell, TX), waste fluid from coal bed methane production (Trinidad, CO), wastewater (Prague, OK) and brine from hydraulic fracturing of shale gas (Dallas-Fort Worth, TX).

[4] Over the last several years, hydraulic fracturing has become widely used in the northeastern United States to extract natural gas from the Marcellus Shale (tight Devonian black shale) [see, e.g., *National Academy of Sciences*, 2012]. Much of the hydraulic fracturing of shale gas has been carried out in Pennsylvania, but the wastewater (brine) from the hydraulic fracturing process is being transported to Ohio and disposed of by injecting into deep wells at a depth range of 2.2–3.0 km under high pressure of up to 17.2 MPa (2500 psi [pounds per square inch]). The target injection intervals are usually sandstone layers in the Knox Dolomite (Lower Ordovician to Upper Cambrian) to Mt. Simon sandstone (Middle Cambrian). Five deep injection wells were drilled in

Additional supporting information may be found in the online version of this article.

[1]Lamont-Doherty Earth Observatory, Columbia University, Palisades, New York, USA.

Corresponding author: W.-Y. Kim, Lamont-Doherty Earth Observatory, Columbia University, 61 Rt. 9W, Palisades, NY 10964, USA. (wykim@ldeo.columbia.edu)


2169-9313/13/10.1002/jgrb.50247

**Table 1.** Recent Potentially Induced Earthquakes Occurring in the United States[a]

| Date | Time | Lat. | Long. | Depth | Magnitude | Location |
|---|---|---|---|---|---|---|
| (year-mo-dy) | (hh:mm:ss) | (ºN) | (ºW) | (km) | ($M_w$) | (references) |
| 2011-11-06 | 03:53:10 | 35.53 | 96.77 | 5 | 5.7 | Prague, OK[b] |
| 2011-08-23 | 05:46:18 | 37.06 | 104.70 | 4 | 5.3 | Trinidad, CO[c] |
| 2011-10-20 | 12:24:41 | 28.86 | 98.08 | 5 | 4.8 | Fashing, TX[d] |
| 2012-05-17 | 08:12:00 | 31.93 | 94.37 | 5 | 4.8 | Timpson, TX[e] |
| 2011-02-28 | 05:00:50 | 35.27 | 92.34 | 3 | 4.7 | Guy, AR[f] |
| 2011-09-11 | 12:27:44 | 32.85 | 100.77 | 5 | 4.3 | Snyder, TX[g] |
| 2011-12-31 | 20:05:01 | 41.12 | 80.68 | 5 | 3.9 | Youngstown, OH[h] |
| 2009-05-16 | 16:24:06 | 32.79 | 97.02 | 4 | 3.3 | Dallas-Fort Worth, TX[i] |

[a]Listed according to their magnitudes.
[b]*Keranen et al*. [2013].
[c]*Meremonte et al*. [2002], *Rubinstein et al*. [2012], and *Viegas et al*. [2012].
[d]*Brunt et al*. [2012].
[e]*Brown et al*. [2012].
[f]*Horton* [2012].
[g]*Davis and Pennington* [1989], http://www.eas.slu.edu/eqc/eqc_mt/MECH.NA/20110911122745.
[h]*ODNR* [2012].
[i]*Frohlich et al*. [2011].

the Youngstown, Ohio area since 2010, but only the Northstar 1 injection well was operational during 2011 (Figure 1). Since the Northstar 1 waste disposal well became operational in late December 2010, Youngstown, Ohio has experienced small earthquakes. On 17 March 2011, residents in Youngstown, Ohio felt a $M_w$ 2.3 earthquake. By 25 November 2011, nine earthquakes ($M_w$ ~1.8–2.8) occurred near Youngstown, Ohio. These shocks are reported by the Division of Geological Survey of the Ohio Department of Natural Resources (ODNR) [see *Ohio Department of Natural Resources (ODNR)*, 2012, Table 5] by using data from sparse seismic stations in the region [*Hansen and Ruff*, 2003]. Prior to 2011, no earthquakes were recorded around Youngstown [*Stover and Coffman*, 1993; *Hansen*, 2012]. Although these earthquakes could not be accurately located due to sparse coverage of seismic stations in the region, these shocks were occurring close to a deep waste injection well Northstar 1 (Figure 1). On 1 December 2011, Lamont Cooperative Seismographic Network deployed four portable seismographic stations around Youngstown at the request of and in collaboration with ODNR to monitor seismicity at close distances and to determine hypocenters of the small earthquakes accurately for assessing whether these shocks were induced by the deep waste disposal well injecting fluid since the end of 2010 in the area (see Figure 1).

[5] On 24 December 2011, a magnitude 2.7 shock occurred in the epicentral area, which was well recorded by the four-station local network in the distance range from 1.9 to 6.5 km from the epicenter. The hypocenter of the shock was very well determined by the local station data, which had adequate coverage with the station azimuthal gap of 119° and distance to the two closest stations less than the focal depth. The shock was located about $0.8 \pm 0.4$ km west of the Northstar 1 well at a focal depth of $3.6 \pm 0.8$ km (95% confidence level). On 30 December 2011, ODNR requested the operator to shut down the Northstar 1 well, because the 24 December 2011 event was located close to the injection well with high confidence. On 31 December 2011 at 20:05 (UTC), a magnitude $M_w$ 3.9 earthquake occurred in the same epicentral area within 24 h from the shutdown of the injection operation.

[6] This is a rare case of likely induced seismicity in the northeastern United States where major events in a sequence have been well recorded by local portable seismographs in place (with a high sample rate of up to 500 samples/s), providing an opportunity to study the sequence of seismicity in detail. In this study, we analyzed the spatiotemporal distribution of seismicity in detail and compared it with available fluid injection parameters to determine if the seismicity in Youngstown area during January 2011 to February 2012 was triggered by the fluid injection into a deep well or not. We also analyzed seismic data in detail in an attempt to shed light on relations between the induced seismicity and physical injection parameters of the deep well injection in the Youngstown area. The *study area* or *Youngstown area* refers to an area about 15 km radius from the main shock on 31 December 2011 (41.118°N, 80.692°W) around Youngstown, Ohio (Figure 1) [see *ODNR*, 2012, Figures 20 and 22].

## 2. Geologic and Geohydrologic Setting

[7] The study area (northeast Ohio around Youngstown) is located in a stable continental region of North America. Subhorizontal Paleozoic sedimentary strata composed of carbonates, evaporates, shale, sandstone, and siltstone of approximately 2.7 km thickness overlies the Precambrian basement. The bedrock units of the study area dip gently (~1°) to the southeast into the Appalachian Basin [*ODNR*, 2012]. The Precambrian crystalline basement in northeast Ohio is composed of igneous and metamorphic rocks, extending the ~1.1 billion years old Grenville Province exposed to the north in Canada. Geologic structures, including faults, pervasive in the Grenville terrain, are considered as the origin of many faults and general structures within the overlying sedimentary strata [*Baranoski*, 2002].

[8] Most known fault systems in the study area trend ESE-WNW [*Baranoski*, 2002]. The Smith Township fault, located about 20 km southwest of the study area, is the closest known fault system, which is a northwest-southeast oriented fault with the upthrown side to the northeast [*Baranoski*, 2002, Map PG-23]. This fault can be mapped on multiple units from the Precambrian surface through the Berea Sandstone (Late Devonian) and above based on well logs and driller's reported formation tops, illustrating that it has had recurrent movement throughout geologic

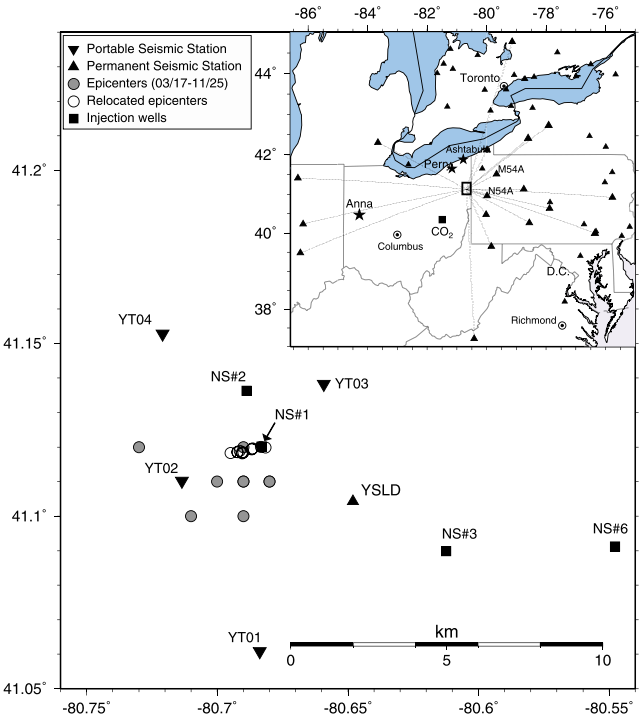


**Figure 1.** Nine earthquakes that occurred in Youngstown area during March–November 2011 are plotted by solid circles. These shocks were reported by ODNR and are scattered around the area. Twelve relocated earthquakes that have occurred in the area during March 2011 to January 2012 are plotted with open circles. The relocated earthquakes include $M_w$ 2.7 shock on 24 December 2011, $M_w$ 3.9 shock on 31 December 2011, and $M_w$ 2.1 shock on 13 January 2012, which are recorded by local portable stations, and hence, located accurately by seismic data. Four portable seismographic stations deployed during 01 December 2011 to 30 April 2012 are plotted with inverted triangles, and a new seismographic station YSLD (Youngstown State University) an ANSS NetQuake strong motion instrument (solid triangle) are plotted for reference. Deep injection wells in the area are plotted with solid squares. Only Northstar 1 (NS#1) was operational during 2011. (inset) Permanent seismographic stations whose data were used to locate small earthquakes around Youngstown, Ohio are plotted with (solid triangles). Stations used for focal mechanism inversion are indicated by their source-receiver paths. Anna indicates Anna western Ohio seismic zone; Perry denotes 31 January 1986 M 5 earthquake; $CO_2$ denotes $CO_2$ No. 1 Well in Tuscawara County; Ashtabula denotes location of 1987 and 2001 earthquakes which occurred near the town.

time [*ODNR*, 2012]. Recent earthquakes that occurred in northeast Ohio with well-determined focal mechanisms indicate that left-lateral strike-slip faulting along E-W trending, steeply dipping faults are the predominant style of faulting due to broad-scale ENE-WSW trending horizontal compression, $\sigma_{Hmax}$ [*Nicholson et al*., 1988; *Zoback and Zoback*, 1991; *Du et al*., 2003; *Seeber et al*., 2004].

[9] The earthquakes in this study occurred exclusively in the Precambrian crystalline basement, whereas the potential reservoir strata in the injection interval are Paleozoic sedimentary rocks of alternating sandstone and dolomite layers. The Northstar 1 well was drilled into Precambrian granite for a total depth of 2802 m. The production casing was cemented in at a depth of 2504 m, and the well was completed open hole to depth 2802 m. Open hole electric logs indicate that the two largest porosity zones within the open hole section are the B zone Sandstone of the Knox Dolomite Group (Ordovician) with a total of 9.8 m net thickness averaging 9.4% porosity and the Mt. Simon Sandstone (Basal Sandstone) of Conasauga Group (Cambrian), which showed 15 m net thickness averaging 10.3% porosity [*ODNR*, 2012]. These two high-porosity zones are considered the reservoirs for brine injection at the site, although the target fluid injection zone is the entire open hole section of the well ~298 m (depth interval between 2504 and 2802 m).

[10] Within the Northstar 1 well, the Precambrian was encountered from a depth of 2741 m through total depth of 2802 m. Just above and at the Precambrian unconformity surface, porosity and permeability zones are indicated on the geophysical logs from 2736 to 2742 m depth. These porosity zones may be due to weathering of the Precambrian unconformity surface [*ODNR*, 2012]. The magnetic resonance log, which can detect higher and lower permeability zones of the rocks, showed a high-permeability zone with a high percentage of moveable fluid in the upper portion of the Precambrian strata (depth 2765–2769 m). Another high-permeability zone with a high percentage of moveable water is found from 2773 to 2776 m. At this same depth, high-angle natural fractures or fault zones have been identified from the well log and images. A clear ENE-WSW trending fracture zone has been identified from compass orientations of natural fractures plotted from fracture and breakout roseplots during geophysical logging at Northstar 1 well [*ODNR*, 2012].

## 3. Seismicity

[11] More than 200 felt earthquakes have been noted in Ohio since 1776, including at least 15 events that have caused minor to moderate damage [*Stover and Coffman*, 1993; *Hansen*, 2012]. The largest and most damaging earthquake occurred on 9 March 1937, in western Ohio, and the M 5.4 shock caused notable damage in the town of Anna, Shelby County, where nearly every chimney in town was toppled. The seismic activity in western Ohio around Anna is relatively frequent compared to other parts of Ohio, and hence, the area is referred to as the Anna seismic zone. A number of earthquakes have occurred in northeast Ohio; for example, M 5.0 event on 31 January 1986 near Perry [*Nicholson et al*., 1988] (see Figure 1), and M 3.8 earthquake on 13 July 1987 and a $M_w$ 3.9 earthquake on 26 January 2001 near Ashtabula [*Seeber and Armbruster*, 1993; *Seeber et al*., 2004]. The 1987 and 2001 earthquakes in Ashtabula have been reported as induced events due to injection of waste fluid at a deep Class I well.

[12] There were no earthquakes reported within the study area (Youngstown, Mahoning County) prior to 2011 [*Stover and Coffman*, 1993]. During 17 March through 25 November 2011, nine small earthquakes ($M_w$ 1.8–2.7) occurred around Youngstown, Ohio (Figure 1). Although, the locations of these shocks were not very accurate due to sparse seismic station coverage, the shocks occurred close to an operating deep waste injection well (Northstar 1 well)

**Table 2.** List of 12 Regional and 9 Local Events Relocated by Using Double-Difference Method[a]

| | Date | Time | Latitude | Longitude | Depth | Mag | Erh | Erz |
|---|---|---|---|---|---|---|---|---|
| Id | (year-mo-dy) | (hh:mm:sec) | (ºN) | (ºW) | (km) | ($M_w$) | (km) | (km) |
| | | | *Twelve Regional Events Located by Regional Seismographic Network* | | | | | |
| 1 | 2011-03-17 | 10:42:20.49 | 41.12008 | 80.68321 | 3.76 | 1.78 | 2.02 | 4.10 |
| 2 | 2011-03-17[b] | 10:53:09.69 | 41.11983 | 80.68148 | 3.84 | 2.28 | 1.61 | - |
| 3 | 2011-08-22 | 08:00:31.55 | 41.11846 | 80.68999 | 3.75 | 2.00 | 1.30 | 2.35 |
| 4 | 2011-08-25 | 19:44:21.36 | 41.11937 | 80.68675 | 3.86 | 2.15 | 2.06 | 3.46 |
| 5 | 2011-09-02[b] | 21:03:26.06 | 41.11960 | 80.68639 | 3.98 | 2.16 | 2.86 | 6.79 |
| 6 | 2011-09-26[b] | 01:06:09.83 | 41.11847 | 80.69048 | 3.77 | 2.33 | 1.22 | 2.57 |
| 7 | 2011-09-30[b] | 00:52:37.57 | 41.11945 | 80.68675 | 3.89 | 2.77 | 1.10 | 2.28 |
| 8 | 2011-10-20 | 22:41:09.96 | 41.11821 | 80.69044 | 3.82 | 2.18 | 1.51 | - |
| 9 | 2011-11-25 | 06:47:27.03 | 41.11885 | 80.69138 | 3.67 | 2.02 | 1.44 | 3.07 |
| 10 | 2011-12-24[b] | 06:24:57.98 | 41.11850 | 80.69235 | 3.56 | 2.66 | 0.38 | 0.84 |
| 11 | 2011-12-31[b] | 20:05:00.04 | 41.11855 | 80.69215 | 3.67 | 3.88 | 0.41 | 0.86 |
| 12 | 2012-01-13 | 22:29:34.00 | 41.11828 | 80.69484 | 3.65 | 2.09 | 0.34 | 0.82 |
| | | | *Small Events Located by Local Portable Seismographic Network* | | | | | |
| 13 | 2012-01-11 | 21:29:28.06 | 41.12294 | 80.67929 | 3.50 | 0.39 | 0.41 | 1.08 |
| 14 | 2012-01-12 | 03:01:45.43 | 41.12304 | 80.68028 | 3.57 | 0.07 | 0.41 | 1.10 |
| 15 | 2012-01-13 | 01:47:29.55 | 41.12252 | 80.68132 | 3.47 | −0.05 | 0.43 | 1.34 |
| 16 | 2012-01-14 | 12:53:36.94 | 41.1203 | 80.6837 | 3.90 | 0.09 | 0.46 | 0.84 |
| 17 | 2012-01-17 | 02:25:59.60 | 41.11901 | 80.69127 | 3.91 | 0.34 | 0.43 | 1.01 |
| 18 | 2012-01-17 | 07:09:08.73 | 41.12413 | 80.67020 | 3.61 | −0.06 | 0.46 | 1.37 |
| 19 | 2012-01-18 | 12:12:01.21 | 41.11866 | 80.69570 | 3.59 | 0.41 | 0.41 | 0.86 |
| 20 | 2012-01-22 | 12:06:20.37 | 41.12316 | 80.67916 | 3.53 | −0.11 | 0.41 | 1.10 |
| 21 | 2012-02-11 | 06:47:19.09 | 41.12459 | 80.67278 | 3.66 | −0.40 | 0.53 | 1.49 |

[a]Event #16 was not relocated by double-difference method; Events 10, 11, and 12 are also relocated by using local seismographic network data; Mag = moment magnitude; Erh = horizontal location error; Erz = vertical location error; Location errors are from single event locations and correspond to 95% confidence error ellipse.
[b]Felt earthquakes.

located in Youngstown. The error ellipses of these shocks were up to 1.99 × 1.57 km at 68% confidence level as reported by ODNR (M. Hansen, personal communication, 2011). Hence, these shocks were suspected as induced earthquakes. The seismicity continued, and on 24 December 2011, a magnitude 2.7 shock occurred in the study area, which was followed by a $M_w$ 3.9 event on 31 December 2011. The $M_w$ 2.1 event on 13 January 2012 was the last $M_w > 2.0$ earthquake of the 2011–2012 sequence (Table 2).

### 3.1. Single Event Location and Location Accuracy

[13] Twelve regional events with $M_w \geq 1.8$ that occurred during 17 March 2011 to 13 January 2012 in Youngtown area were first located by using HYPOINVERSE [*Klein*, 2007]. The velocity model used for location is an average 1D model for northeastern Ohio that consists of the top layer with *P* wave velocity of 4.5 km/s and thickness of 2.7 km, and a 7.3 km thick crystalline basement with *P* wave velocity of 6.12 km/s [*Seeber et al*., 2004]. The *S* wave velocities are considered to be $V_P/\sqrt{3}$ (Table 3). All events were located with *P* and *S* wave arrival times from at least a dozen seismographic stations around Youngstown, Ohio. For the nine earthquakes during March–November 2011, the nearest station is at about 60 km, but most stations were at distances 100 to 300 km with azimuthal gap of about 90° (Figure 1); hence, the location uncertainties are large—horizontal error is up to 2.8 km for 95% confidence level as listed in Table 2. The locations of 12 earthquakes with their horizontal error ellipse are plotted in Figure 2.

[14] The last three events among the 12 shocks were also recorded by a four-station local network deployed during 1 December 2011 to 30 April 2012 around the epicentral area (Figures 1 and 2). Hence, these shocks were accurately located by the local network data. Three shocks exceed the network criteria [e.g., *Gomberg et al*., 1990], which are based on the geometry of stations, and can be used to assess the reliability of the location. For three shocks, the number of local *P* or *S* wave arrival times used for each event were greater than eight (nobs = 8–10) of which half are *S* wave arrivals; the greatest azimuthal gap without observation was less than 180° (gap = 90–120°); distance to the closest station was less than focal depth (dmin = 1.9 km); and at least one *S* wave arrival time was within a distance of about 1.4 times the focal depth for good depth constraint [*Gomberg et al*., 1990]. Three earthquakes that were recorded both by regional and local networks provide data to assess the event location uncertainty and will be used in a later section to anchor relocation of earlier shocks with no local data coverage.

[15] To assess the effect of vertical velocity heterogeneities on focal depth and epicenter determination, we constructed 1D Earth models from the available acoustic well logs in the study area (NS#1 and $CO_2$ No. 1 Well, see Figure 1). We inferred crustal velocity structure for the top 2.74 km of Paleozoic sedimentary rocks in the region (see the supporting information). The Youngstown well log velocity model consists of 19 layers and is characterized by interbedded high-velocity carbonate rock layers and thick low-velocity shale strata. The prominent strata are the Salina Group of Upper Silurian formation with interbedded salt, anhydrite, dolomite, and shale, which show large velocity and density fluctuations, followed by Lockport Dolomite of Lower Silurian that exhibit very high *P* wave velocity (see Figure S1). At the injection target interval depth

**Table 3.** Youngstown, Ohio Layered Earth Models

| Depth | $V_P$ | $V_S$ | Depth | $V_P$ | $V_S$ | Density | Depth | $V_P$ | $V_S$ | Density | $V_P/V_S$ |
|---|---|---|---|---|---|---|---|---|---|---|---|
| (km) | (km/s) | (km/s) | (km) | (km/s) | (km/s) | (kg/m$^3$) | (km) | (km/s) | (km/s) | (kg/m$^3$) | |
| *Northeastern Ohio*[a] | | | *Youngstown well log A*[b] | | | | *Youngstown well log B*[c] | | | | |
| 0.00 | 4.50 | 2.60 | 0.00 | 3.86 | 2.19 | 2630 | 0.00 | 3.86 | 2.26 | 2630 | 1.71 |
| | | | 0.93 | 4.98 | 2.83 | 2600 | 0.93 | 4.98 | 2.80 | 2600 | 1.78 |
| | | | 2.11 | 6.13 | 3.48 | 2710 | 2.11 | 6.13 | 3.50 | 2710 | 1.75 |
| 2.74 | 6.12 | 3.54 | 2.74 | 6.15 | 3.49 | 2710 | | | | | |
| 10.0 | 6.62 | 3.83 | 10.0 | 6.62 | 3.76 | 2710 | 10.0 | 6.62 | 3.83 | 2710 | 1.73 |

[a]Constant $V_P/V_S = 1.73$ and density = 2700 kg/m$^3$.
[b]Constant $V_P/V_S = 1.76$.
[c]Variable $V_P/V_S$. The Moho is at 41 km depth with $V_P = 8.1$ km/s, $V_S = 4.68$ km/s, and density = 2700 kg/m$^3$; at the top of the upper mantle.

range of 2.3–2.74 km, low-velocity sandstone and high-velocity dolomite strata are interbedded.

[16] In order to assess uncertainties in earthquake location, we inferred a simple average 1D velocity model by averaging groups of strata with similar characteristics. Hence, the model Youngstown well log A has three layers with constant $V_P/V_S$ ratio of 1.76, and a two-layer model Youngstown well log B has various $V_P/V_S$ ratio for each layer (Table 3). Locations using these velocity models indicate that two layers over the basement Youngstown well log B model, with variable $V_P/V_S$ ratios for each layer, yielded the location with the least root-mean-square (RMS) travel time residuals; however, the differences in location parameters are negligible. The northeastern Ohio velocity model that we used yields the focal depths of 3.52, 3.67, and 3.64 km for 24 December 2011, 31 December 2011, and 13 January 2012 events, respectively, with their 95% confidence error ellipsoids extending up to 0.86 km in the vertical direction. The horizontal error is up to 0.41 km at 95% confidence level (see Table 2).

[17] Three different velocity models yield very similar locations with negligible differences in their location errors. The differences in focal depths are less than 0.15 km depending upon the three models used. If we take the centroid of the source region to be at 3.5 km depth, then these location uncertainties in the vertical direction stretch between 2.7 and 4.3 km depths, which puts the earthquake sources firmly in the Precambrian basement. We consider the location accuracy given is well constrained by velocity structure from well log data, and the solution is reliable considering the network criteria discussed above.

### 3.2. Focal Mechanism of the Earthquake on 31 December 2011

[18] The shock on 31 December 2011 was large enough to allow us to determine its seismic moment, focal mechanism, and focal depth by modeling observed seismic records at permanent seismographic stations around the study area and inverting for these parameters (Figure 1). We employed a regional waveform inversion method described in *Kim and Chapman* [2005], which is essentially a grid search inversion technique over strike (θ), dip (δ), and rake (λ) developed by *Zhao and Helmberger* [1994]. The results of the waveform modeling and inversion indicate that the focal mechanism of the main shock on 31 December 2011 shock is predominantly strike-slip faulting along steeply dipping nodal planes (see Figure 3). The best fitting double-couple source mechanism parameters are θ = 265°, δ = 72°, λ = 12° (second nodal plane; θ = 171°, δ = 79°, and λ = 162°), and seismic moment, $M_0 = 8.30 \pm 8.0 \times 10^{14}$ Nm ($M_w$ 3.88). The subhorizontal *P* axis trends southwest-northeast (219°) with a plunge of 5° whereas the *T* axis trends SE-NW (127°) with a plunge of 20°. The *P* axis orientation is about 15° rotated counterclockwise from that of the 26 January 2001 earthquake in Ashtabula, Ohio, which is the nearest earthquake with known focal mechanism [*Du et al*., 2003]. The waveform modeling indicates that the synthetics calculated for focal depth of 3 ± 1 km fit the observed data well.

### 3.3. Accurate Relocations of 12 Regional Earthquakes

[19] We relocated 12 regional earthquakes by using the double-difference earthquake relocation method to minimize the effect of velocity model errors [*Waldhauser and Ellsworth*,

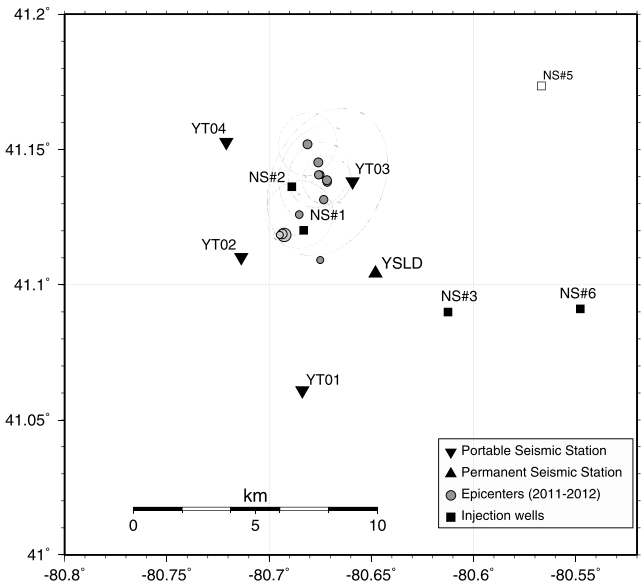


**Figure 2.** Single event locations of the 12 regional earthquakes that occurred in Youngstown, Ohio during March 2011 to January 2012 are plotted with shaded circles. The horizontal location errors are represented by 95% confidence error ellipses. Four portable seismographic stations around the region deployed during 01 December 2011 to 30 April 2012 and a new seismographic station YSLD (Youngstown State University) are plotted for reference. The last three events were located by using *P* and *S* wave readings from four portable seismographic stations located within 2–6.5 km from the earthquake source area.

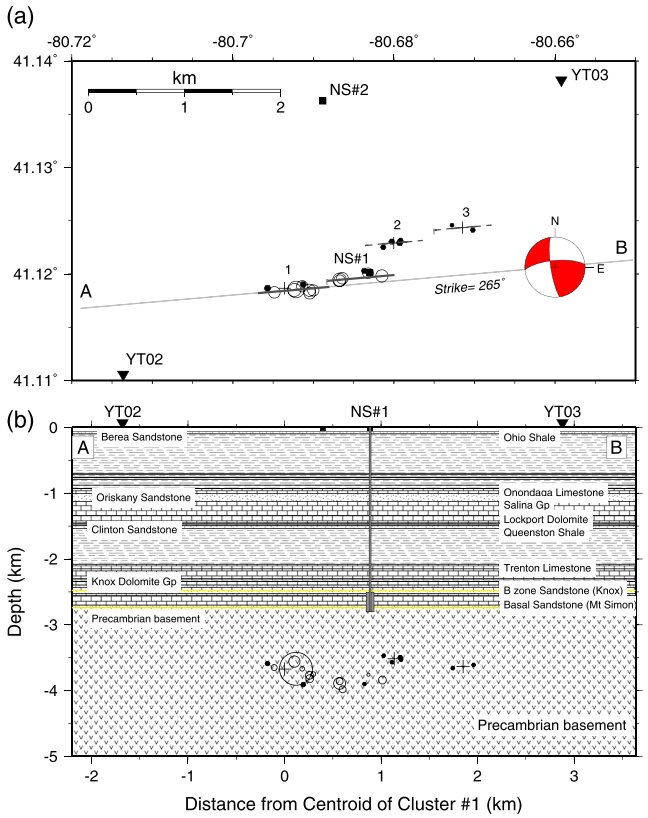


**Figure 3.** (a) Relocated 12 regional earthquakes (circles) and 9 local earthquakes (black hexagons) which occurred during 17 March 2011 to 18 February 2012. Earthquakes are relocated in three clusters. Focal mechanism of the $M_w$ 3.9 shock on 31 December 2011 is represented by a beachball indicating predominantly a left-lateral strike-slip faulting mechanism. Line A-B is parallel to the trends of the earthquake distribution striking N85°. Deep injection wells in the area NS#1 and NS#2 are indicated (solid squares) and portable seismographs YT02 and YT03 are plotted with solid inverted triangles. Centroid of clusters is plotted with plus symbols. (b) Geologic section along A-B at NS#1. Most of the rocks above the crystalline Precambrian basement are Paleozoic strata that consist of sandstone, limestone, shale, and dolomite. The injection well, NS#1, is indicated with a vertical shaded bar down to a depth of 2802 m. Open section of the well between 2504 and 2802 m is indicated by shaded rectangle. Target injection zone is between B zone sandstone of the Knox Dolomite Group and Mt. Simon sandstone (basal sandstone). Hypocenters are plotted with open circles, whose size is proportional to source radius of each event determined by empirical Green's function analysis and circular source model of *Madariaga* [1976].

2000]. We employed the waveform cross-correlation technique to reduce arrival time picking errors of weak regional *P* and *S* wave arrivals. The relocated regional events show that the epicenters align along a trend striking ENE-WSW (N85°) and at focal depths from 3.5 to 4.0 km (see Table 2 and Figure 3). Hence, these regional events are within a 1.2 km long near-vertical en echelon fault just below the Northstar 1 wellbore (Figure 3). A geologic section along the line A-B below the Northstar 1 well shown in Figure 3 indicates that all the events occurred in the Precambrian basement. Distribution of the main shock and other shocks suggest that the nodal plane striking 265° and dipping 72° to North is the likely fault plane and that the mechanism is left-lateral strike-slip faulting along E-W trending subsurface faults.

### 3.4. Small Earthquakes Located by Portable Seismograph Data

[20] Nine small earthquakes with magnitude $M_w$ −0.40 and 0.41 were detected and located by the four-station local network during 11 January to 11 February 2012 (Table 2). We relocated these nine events by using the double-difference earthquake relocation method with the waveform cross-correlation technique to reduce arrival time picking errors. The accurate relocation shows that the epicenters align into three distinct clusters (Figure 3). Three events are located in cluster #1 (events #16, #17, and #19), whereas four small events are in cluster #2 (events #13, #14, #15, and #20) and two small events are in cluster #3 (events #18 and #21; Figure 3). The cross sections of the clusters indicate that hypocenters of these shocks are at focal depth between 3.5 and 3.9 km and on near-vertical en echelon faults trending ENE-WSW (N85°; Figure 3), which is consistent with the locations of 12 regional events.

### 3.5. Regional Seismicity and Magnitude Distribution

[21] The distribution of felt earthquakes as well as small shocks detected and located by local network data in Youngstown suggests that there must have been a number of small shocks (less than $M \leq 2.0$) in the area that may have been undetected by the sparse regional seismic network. We applied a waveform correlation detector using the regional station data to detect those small shocks. The correlation detector is known to lower the seismic event detection threshold by about 1.0 magnitude unit beyond what standard processing detects [e.g., *Schaff*, 2008; *Schaff and Waldhauser*, 2010; *Gibbons and Ringdal*, 2012]. The method is well suited for this study, as we are dealing with small and repeating shocks with similar waveforms located within about a quarter wavelength from each other. We detected 97 additional small earthquakes ($0.4 < M_w < 1.8$) that occurred within about 1 km from the main shock during January 2011 to May 2012 by using the multichannel correlation detector. Hence, the method was able to find additional events by a factor of 10 increase in number of events such as those predicted by the Gutenberg-Richter magnitude-frequency relation. Three-component records from two USArray stations, M54A ($\Delta = 56$ km) and N54A ($\Delta = 107$ km) were the most useful (Figure 1). Three-component waveform records of 24 December and 31 December 2011 shocks were used as master templates.

[22] Figure 4 shows all detected seismic events plotted with their occurrence date against moment magnitude of the events, since commencement of the fluid injection on 29 December 2010 until the end of January 2012. A total of 109 earthquakes with magnitude between $M_w$ ~0.4 and 3.9 detected by the correlation detector are plotted with solid bars, whereas 58 small earthquakes with magnitude $0.0 \leq M_w < 1.0$ detected by the local network are plotted with red bars. Among the 58 shocks, only four events were located by the local network data, as 54 events were only detected by a single station (YT01) which was the only station recording

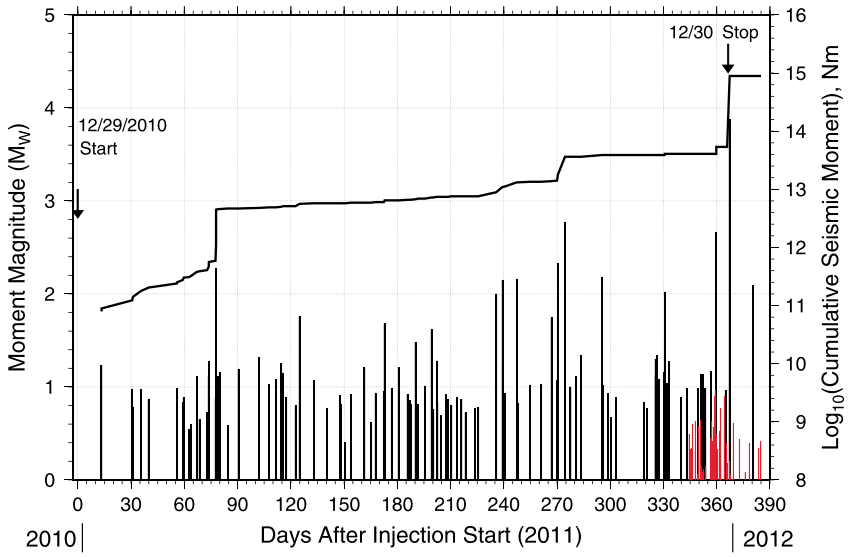


**Figure 4.** Earthquakes that occurred during 29 December 2010 to January 2012 in Youngstown area are plotted by vertical bars against their occurrence date, whose lengths are proportional to their moment magnitude, $M_w$ (left vertical axis). Small earthquakes that occurred during December 2011 to January 2012 that are only recorded by local portable stations are plotted with red bars. Cumulative seismic moment is plotted by a continuous solid line (right vertical axis). The cumulative moment release is dominated by a few large ($M_w \geq 2.5$) events.

continuously during December 2011. Moment magnitudes ($M_w$) of earthquakes that occurred in the Youngstown area were determined from RMS (root-mean-square) amplitude of *S* or *Lg* waves and calibrated to that of the $M_w$ 3.88 main shock on 31 December 2011 [*Shi et al*., 2000]. For 58 small shocks, moment magnitudes were determined by using peak amplitude of *S* arrivals scaled to that of the main shock.

[23] These shocks might have been related to the fluid injection operation, and their spatiotemporal distribution can help us to understand the relationship between the injection parameters and induced seismicity in the area. Cumulative seismic moment of 167 earthquakes with $M_w$ 0.0–3.9 is plotted against occurrence date as a thick continuous line in Figure 4. The seismic moment release is dominated by a few large ($M_w > 2.5$) earthquakes (Figure 4). We estimate that the detection threshold for the regional earthquakes using the correlation detector is about $M_w$ 1.0 in the Youngstown, Ohio region, whereas the detection threshold for local earthquakes in the study area is about $M_w \geq -0.5$ by using local network data.

## 4. Waste Fluid Injection at Northstar 1 Deep Well, Youngstown, Ohio

[24] The Northstar 1 well was drilled to a total depth of 2802 m, and the waste fluid injection commenced on 29 December 2010. Daily injection volumes and start injection pressures are plotted in Figure 5 for the entire fluid injection operation [*ODNR*, 2012]. The maximum surface injection pressure was 13.0 MPa (=1890 psi) based upon the actual specific gravity of the injection fluid. The maximum injection pressure was permitted to increase up to 15.5 MPa on 16 March 2011 and increased to 17.2 MPa on 3 May 2011 [*ODNR*, 2012]. Three episodes of injection pressure changes are indicated in Figure 5. In the first 60 days, the fluid injection was carried out with a low level of injection pressure ~5 MPa, and the injection volume was less than 100 $m^3$/day. The injection parameters slowly increased with the injection pressure of about 10–12 MPa, and the daily injection volume of about 100–200 $m^3$/day during the days 60–110 (Figure 5). During days 110–140, the injection pressure increased sharply to 15.5 MPa and consistently held, and injection volume exceeded 300 $m^3$/day (Figure 5). The fluid injection at the well reached operational injection pressure of 17.2 MPa and injection volume of about 320 $m^3$/day around 19 May 2011 (day 141; Figure 5). These injection parameters are kept during June through December 2011 (see Figure 5).

[25] We can recognize several instances of gaps in surface injection pressure—a sudden drop in injection pressure followed by prolonged low pressure. These gaps are present in the daily injection volumes as well (Figure 5). The drops in injection pressure correspond to 2–4 days of no pumping at the wellhead followed by 8 to 20 days of gradual increase of injection pressure (Figure 5). Most of the short and sharp pressure drops correspond to no pump running for a day on national holidays—Memorial Day, 4 July, and among others. The longer gaps are due to injection tests, on Labor Day (246–250), pump maintenance (days 283–285), and Thanksgiving holidays (days 331–334), etc.

[26] The surface injection pressures shown in Figure 5 are listed as *average pressure* in the Northstar 1 injection log, which lists average wellhead pressure between start pressure at the beginning of injection each day and stop pressure at the end of injection each day. The wellhead pressure drops substantially after days of no injection operation as shown as minima in the pressure plot (Figure 5). Dissipation of injection pressure during the gaps is estimated to be about 0.069 MPa/h drop in the wellhead pressure. The average injection rate (number of hours the pump ran over a total daily injection volume) was about 15 $m^3$/h and remained nearly constant over the whole year

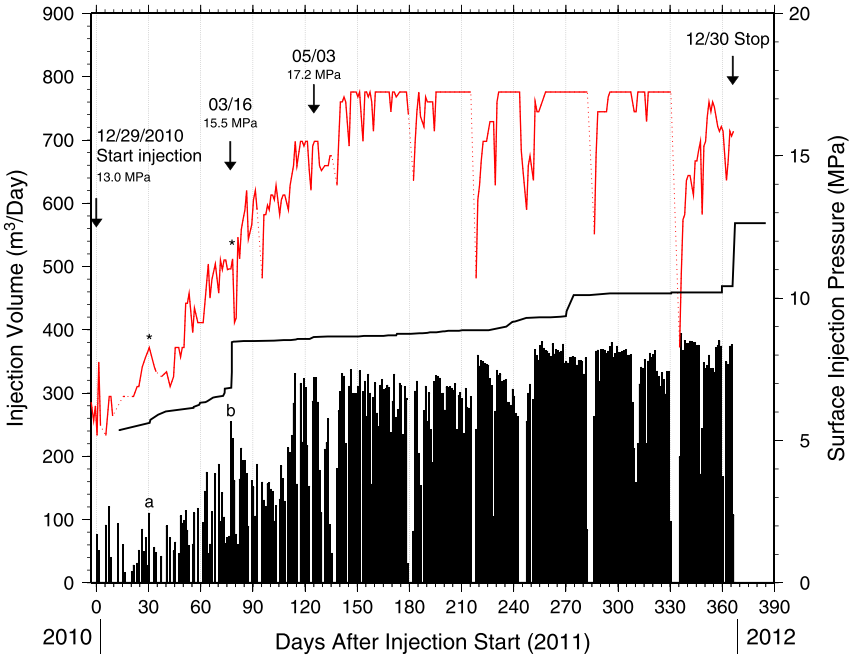


**Figure 5.** Average surface injection pressure in each day at Northstar 1 well during its operation 29 December 2010 to 30 December 2011 in MPa is plotted with red line (right vertical axis). Dotted portions indicate no entries in the injection log. Daily total injection volume in cubic meters, $m^3$, is plotted with solid bars (left vertical axis). Average injection volume is about 350 $m^3$/day when the well is running full time at the maximum surface injection pressure of 17.2 MPa. A total of 78,797.6 $m^3$ of fluid have been injected into the Northstar 1 well. Cumulative seismic moment of 167 earthquakes that occurred during the fluid injection period is plotted as continuous solid line for reference. Instances of sharp increase of daily injection volume are indicated **a** and **b**, which correspond to occurrence of earthquakes (see the text).

of injection operation at Northstar 1 well. During the summer months, June–August, the injection rate was somewhat low at 12.6 $m^3$/h.

[27] On 30 December 2011, ODNR requested the operator of the Northstar 1 cease injection at the well based upon the proximity of the 24 December 2011 hypocenter to the Northstar 1 injection wellbore. As of 31 December 2011, a total of 78,797.6 $m^3$ (495,622 barrels) of fluid had been injected into the Northstar 1 well. It is the only well out of 177 class II (brine disposal) waste disposal wells operating in the state of Ohio during 2011 that has been linked to potentially induced earthquakes. Daily total injection volume is proportional to the product of pump run time and injection pressure, and it may be an appropriate parameter to assess the effect of fluid injection on the subsurface hydraulic system (injection interval). The injection pressure alone is not sufficient to represent the injection; it needs sufficient fluid to exert the pressure on subsurface rocks.

### 4.1. Peaks and Minima of Injection Parameters and Seismicity at Youngstown, Ohio

[28] When the seismicity in the Youngstown area during 2011–2012 is compared with the fluid injection parameters at the deep injection well Northstar 1, there is some correlation between the injection parameters and occurrence of earthquakes. No felt earthquakes occurred prior to the injection operation on 29 December 2010. Once the injection at the well commenced, and the injection pressure was slowly applied, the first earthquake of $M_w$ 1.2 occurred on 11 January 2011 at 11:16, about 13 days after the commencement. As the fluid injection progressed and injection parameters steadily increased, the seismicity in the area also increased as shown in the cumulative seismic moment release from days 13 to 76, 2011 (Figure 5). The seismicity shown in Figure 4, in particular, the cumulative moment closely follows the increased surface injection pressure as well as injection volume (Figure 5).

[29] There are a pair of peaks in injection volumes as marked **a** and **b** in Figure 5. These sharp peaks in the injection flow rate ($m^3$/day) appear to be correlated to the occurrence of earthquakes that followed such sharp increases closely. Such a short-term—several hours to a few days—response of the injection medium to the fluid injection may be an indication that the injection target strata are highly fractured, and the storage volume is hydraulically connected to the injection fluid dissipation pathways. The cross correlation between the earthquake series and the fluid pressure as well as injection flow rate series were calculated to determine whether there was a lag between peak fluid pressure and peak seismic activity. The cross correlation is not symmetrical and indicates that the peak of seismicity follows the peak pressure by approximately five days. The lack of symmetry in the cross correlation is due to delayed seismic activity at the beginning and continued seismic activity after the injection of fluid. About 10+ days of short-term response is also reported at RMA [*Healy et al.*, 1968] and is suggested that it was due to fractured Precambrian crystalline bedrock at the site. Although, the Precambrian basement in the Youngstown area was not the primary target interval, the fractured Precambrian rock directly below the wellbore shares similar fractured reservoir characteristics as the RMA site.

#### 4.1.1. Quiescence of Seismicity and Minima of Fluid Injection Pressure

[30] There are quiescences in seismicity during certain time intervals such as days: 285–296 and 305–320 (see Figure 4), as marked with yellow bars in Figure 6. Those quiescent periods are defined as time intervals at least four consecutive days without earthquakes ($M_w \geq 0.9$), and they appear to follow the minima in the injection pressure as represented by vertical red lines in Figure 6. Although not all the injection pressure minima correlate with the quiescence in seismicity, 75% of the pressure minima (18 out of 24 minima) fall within the quiescent intervals (Figure 6), whereas about 62% of the quiescent intervals (18 out of 29 intervals) are associated with the pressure minima (Figure 6). We suggest that the cessation of fluid injection may have caused quiescences of earthquakes as illustrated in Figure 6. We are unable to model such behavior with reservoir analysis due to lack of detailed knowledge on the ambient pore pressure at the Northstar 1 well [e.g., *Hsieh and Bredehoeft*, 1981].

### 4.2. Physical Basis of the Induced Seismicity in Youngstown, Ohio

[31] The basic mechanism for initiation of induced earthquakes during fluid injection into deep wells is well understood [e.g., *Hubbert and Rubey*, 1959; *Healy et al*., 1968; *Raleigh et al*., 1976]: tectonic strain stored in the basement rock is released via earthquakes that are triggered by the injection of fluid into the basement rock. The Mohr-Coulomb fracture criterion may be written as [*Healy et al*., 1968; *Yeats et al*., 1997]:

$$\tau = \tau_0 + \mu \sigma_n, \tag{1}$$

where $\tau$ is the shear stress on the fault plane at failure, $\tau_0$ is the fracture cohesion, μ is the coefficient of friction, and $\sigma_n$ is the effective normal stress. Under the presence of pore pressure, the effective normal stress consists of two parts, a pore pressure $P$ and the total stress $S$; hence, $\sigma_n = (S_n - P)$, in which $S_n$ is the total normal stress acting on the fault plane, and $P$ is the pressure of the ambient fluid [*Healy et al*., 1968]. For fault slip on preexisting faults, the cohesive strength ($\tau_0$) is taken to be close to zero [*Zoback and Healy*, 1984; *Zoback*, 1992]. $\mu$ ranges from 0.6 to 1.0 [*Zoback and Townend*, 2001], and *Byerlee* [1978] reports $\mu = 0.85$ for a variety of rock types at normal stress up to 200 MPa. The right side of the equation consists of a frictional term $\mu$ $(S_n - P)$, plus the cohesive strength, $\tau_0$ and, hence as long as the right side is greater than the shear stress ($\tau$), fault slip will not occur. This empirical relation indicates that the effect of increasing pore pressure is to reduce the friction resistance to fault slip by decreasing the effective normal stress ($\sigma_n$) acting on the fault plane.

[32] If the area has preexisting weak zones (fractures and faults), and the area is already close to failure, then a small increase in pore pressure would trigger earthquakes. Therefore, the gaps in injection parameters at the Northstar 1 well reduced the pore pressure ($P$) in the above equation and effectively strengthened the friction resistance on the subsurface fault. This leads to reduced size and number of triggered earthquakes and the quiescence in seismicity as shown in Figure 6.

[33] The parameters in the above equation can be evaluated for the Youngstown area on the basis of the following assumptions and relations between $\tau$, $\sigma_n$, and the principal stresses. For strike-slip faulting in Youngstown area, the least ($S_3$) and greatest ($S_1$) principal stresses are horizontal [*Yeats et al*., 1997]. We take the least principal stress ($S_3$) to be the bottom hole pressure (BHP) of 27.5 MPa (=1000 kg/m$^3$ × 9.8 m/s$^2$ × 2802 m); the intermediate principal stress $S_2$ is vertical and equal to the lithostatic pressure (mainly overburden) [*Healy et al*., 1968]. $S_2$ at the bottom of injection well at 2802 m is 74.1 MPa (=2700 kg/m$^3$ × 9.8 m/s$^2$ × 2802 m). The greatest principal stress $S_1$ must be at least 74.1 MPa. Estimates of the pore pressure before the fluid injection ($P$) at the Northstar 1 well is unknown. If we take a similar value to that of RMA well, which was about 75% of the BHP, $P$ is 20.6 MPa (=27.5 MPa x 0.75) which corresponds to the static fluid level of 700 m below the wellhead after injection stopped [*Hsieh and Bredehoeft*, 1981]. From the Mohr failure envelope, the shear and effective normal stresses are given as [*Healy et al*., 1968; *Yeats et al*., 1997]:

$$\tau = \frac{(S_1 - S_3)}{2} \sin 2\alpha \tag{2}$$

$$\sigma_n = \frac{(S_1 + S_3 - 2P)}{2} + \frac{(S_1 - S_3)}{2} \cos 2\alpha \tag{3}$$

where $\alpha$ is the angle between the fault plane and the plane normal to $\sigma_1$. $\alpha \sim 45°$ for the strike-slip focal mechanism with $P$ axis trending 219° and fault plane striking 265° given in the previous section for Youngstown area. Given $S_1 = 74.1$ MPa, $S_3 = 27.5$ MPa, $P = 20.6$ MPa, and $\alpha = 45°$, the shear and effective normal stresses on a potential fault plane are $\tau = 28.3$ MPa and $\sigma_n = 30.2$ MPa. Therefore, according to the Mohr-Coulomb failure criterion, the cohesive strength, $\tau_0$ would have to be at least 2.6 MPa to prevent fault slip in the reservoir rocks in Youngstown area prior to fluid injection. If the cohesive strength is taken to be $\tau_0 = 0$ on the fault plane, then pore pressure ($P$) must be less than ~17.5 MPa to prevent failure.

[34] Average injection pressure of 7.5 MPa for two days and a daily total injection volume of 102 m$^3$/day may have triggered an $M_w$ 1.0 shock on 3 February 2011 (day 35, Figure 6). If we use this injection pressure, the pore pressure is raised to 35.5 MPa (27.5 MPa + 7.5 MPa; BHP plus surface injection pressure), and it yields; $\tau = 28.3$ MPa, $\sigma_n = 15.3$ MPa, and $\tau_0 = 15.3$ MPa. The occurrence of faulting upon reduction of the frictional term due to increased pore pressure indicates a value for $\tau_0$ of 15.3 MPa or less. This is comparable to $\tau_0 = 15.1$ MPa estimated for the RMA [*Healy et al*., 1968]. The cohesive strength for crystalline basement rocks is about 50 MPa [*Healy et al*., 1968]. The cohesive strength of 15.3 MPa may be reasonable for the fractured injection media at the Youngtown area, which appears to be fractured Precambrian rocks with preexisting fault or fracture zones, to hold the fault together.

## 5. Discussion

[35] The earthquakes did not stop immediately after the shutdown of the injection operation at Northstar 1, although the rate and size of earthquakes steadily dropped within a

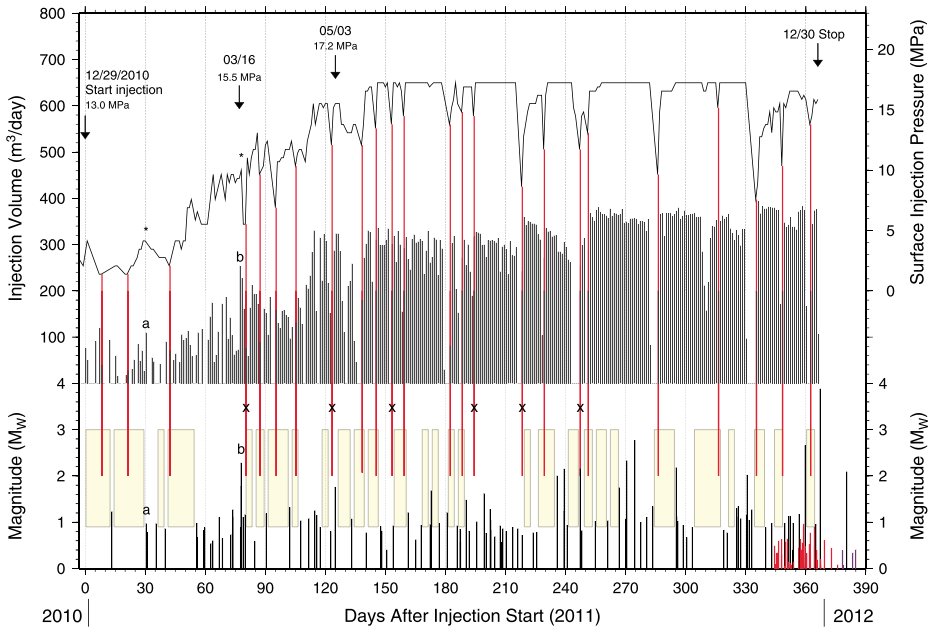


**Figure 6.** Surface injection pressure in MPa in each day during the whole operation of the Northstar 1 well 29 December 2010 to 30 December 2011 is plotted with black line (right vertical axis). Daily total injection volume in cubic meters ($m^3$) is plotted with solid bars (left vertical axis) and the earthquakes that occurred during December 2010 to January 2012 are plotted with vertical bars whose lengths are proportional to their moment magnitude, $M_w$. The minima in the injection pressure are represented by vertical red lines, and quiescent intervals of seismicity are indicated by yellow bars. These injection pressure minima are due to no pumping at the wellhead during equipment services and holidays, and 75% of the minima appear to be correlated to quiescent intervals of seismicity. The minima that are not related to the quiescent intervals are marked by x.

month following shutdown. The largest shock on 31 December 2011 occurred about 24 h after the end of injection on 30 December 2011 at Northstar 1. The largest earthquakes postdated the end of injection at other sites such as, Ashtabula, Ohio, and RMA near Denver, Colorado. At RMA, the largest earthquake ($M_w$ 5.2) occurred on 10 April 1967 more than a year after injection ceased on February 1966 [*Healy et al*., 1968]. Usually, pore pressure buildup from several months of fluid injection would require time to return to the preinjection level.

### 5.1. Migration of Seismicity From East to West

[36] Twelve relocated regional earthquakes cluster along ENE-WSW (Figure 7a), and their vertical distribution suggests that the rupture area can be represented by a pair of rectangular planes aligned en echelon with overall length of about 1.2 km and width of about 0.5 km (Figure 7b). The linear trend is consistent with a nodal plane striking 265° of the focal mechanism for the main shock on 31 December 2011 (Figure 7a). A pair of earthquakes on 17 March 2011 (events #1 and #2) occurred at the eastern end of a 1.2 km long rupture area close to the wellbore (Figure 7a), then the subsequent shocks in August and September 2011 occurred in the further western part of the rupture area (events #3 through #7; Figure 7). The shocks on December 2011 and January 2012 including the main shock on 31 December 2011 occurred at the western end of the rupture area (events #10–#12; Figure 7). Hence, the seismicity migrated gradually from the eastern end of the fault area close to the injection wellbore toward the western end, away from the injection point (Figure 7).

[37] The west-south-west (WSW) migration of the seismicity from the injection point can be explained by the outward expansion of the high fluid pressure front which increases pore pressure along its path on the fault zone and triggers earthquakes, and the progressive westward migration of seismicity continues until injection stops. The effect of increased pore pressure is to reduce the frictional resistance to faulting by decreasing the effective normal stress across the fracture plane [*Healy et al*., 1968]. A predominantly WSW-ENE trending seismicity with narrow depth ranges of 3.5–4.0 km indicates the existence of a fractured Precambrian rock in the form of en echelon rectangular faults as conduits of fluid migration. A migration of seismicity was also observed at RMA [*Healy et al*., 1968; *Hsieh and Bredehoeft*, 1981]. There is minor seismic activity in the northeast from the injection well within the ENE-WSW trending fractured Precambrian basement, suggesting the existence of step-like en echelon rupture planes (see Figure 3a). Deep basement fault(s) in the study area may act as vertical fluid conduits and provides a hydraulic connection between the fluid disposal well injection depths and the earthquake source depths (Figure 7).

### 5.2. Speed of the Earthquake Migration

[38] The seismicity migrated from East to West for about 1.2 km during 17 March 2011 to 13 January 2012. Although the migration rate is not homogeneous in time, an average speed is about 4.0 m per day (= 1.2 km/300 days) or ~120 m per month. Somewhat higher migration speed of 2 to 40 m/h was observed in a water injection experiment at the Nojima

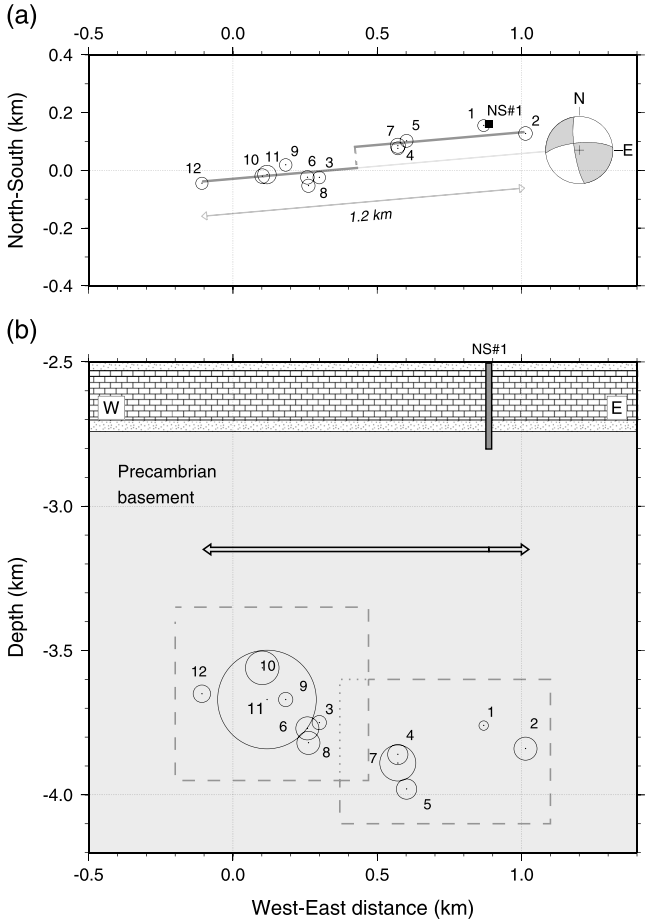


**Figure 7.** (a) Accurately relocated regional earthquakes that have occurred during 17 March 2011 to 13 January 2012 in Youngstown area are plotted by circles and denoted by event ids. The deep injection well Northstar 1 (NS#1) is plotted for reference. Events on 17 March 2011 (#1 and #2) are located close to the injection well. Subsequent later events have occurred further away from the injection well and the events on December 2011 to January 2012 are located at the western end of the rupture zone; (b) Cross-section view of the hypocenters. Injection interval of the well between 2504 and 2802 m is indicated by shaded rectangle. Events are clustered in depth ranges 3.5 to 4.0 km, and the seismicity shows gradual migration from the eastern end close to the injection wellbore to the western end of the fault zone. Circle sizes are proportional to the source radius of each event determined by empirical Green's function analysis and circular source model of *Madariaga* [1976]. Dashed lines suggest possible maximum rupture planes based on source model of *Brune* [1970].

fault zone in Japan [*Tadokoro et al*., 2000, 2005]. *Seeber et al*. [2004] reported a somewhat similar observation in Ashtabula, Ohio where seismicity shifted ~1 km from the point of injection during May 1986 to June 1994.

[39] The seismicity waned after the main shock on 31 December 2011 (which also coincides with the stopping of the injection operation), which is somewhat different from the naturally occurring earthquakes in which most of the aftershocks occur immediately following the main shock. The seismicity plotted in Figure 4 is similar to an earthquake swarm, but in this case, seismicity is spread in time and space due to migrating high fluid pressure front. As such, most events may have occurred as doublets and multiplets.

### 5.3. Total Injected Volume and Maximum Seismic Moment of the Induced Earthquakes

[40] *McGarr* [1976] reported that annual sums of seismic moments for the Denver earthquakes from 1962 to 1965 agree with the yearly total moment estimated from the volume of fluid injected at the RMA well. He postulated that the seismicity that results from a change in volume $\Delta V$ is related to the sum of the seismic moments of the earthquake population, $\Sigma M_0$, that is, $\Sigma M_0 \sim \nu |\Delta V|$, where $\nu$ is the rigidity, and a necessary condition is that the change in volume is accommodated only by seismic failure. *Gibbs et al*. [1973] reported that the number of earthquakes per year appeared to correlate with changes in the quantity of fluid injected per year during 1962–1970 in Rangely, Colorado.

[41] *McGarr* [2012] proposed that the maximum induced earthquake size (moment) scales with total volume of injected fluid. The pore fluid pressure from injection is needed to trigger the earthquakes [*Raleigh et al*., 1976; *Zoback and Harjes*, 1997], but additionally the total injected volume must be large enough to exert fluid pressure over a sufficiently large area of the preexisting faults, thereby triggering large-sized earthquakes. However, even if this volume is large, it may not be necessary that earthquakes will occur. For example, if a large volume is injected over a long period of time, sufficient to achieve fluid migration, earthquakes may not be triggered. We conclude that although total injected volume is a readily available parameter that may be useful for assessing the propensity for earthquakes to occur, it may need to be interpreted in association with knowledge of the injection rate, and/or an assessment of pressure levels. As in the progressive migration of seismicity, more injected volume would have a better chance to exert pressure to a wider rupture area, thereby increasing the maximum size of the induced earthquakes. Although we do not know the WSW-ENE extent of the fault(s) in the Youngstown area, it is possible that continued injection of fluid at Northstar 1 well could have triggered potentially large and damaging earthquakes.

## 6. Summary and Conclusions

[42] A total of 167 small earthquakes ($M_w$ 0.0–3.9) were detected during January 2011 to February 2012 in Youngstown, Ohio. These shocks were located close to a deep fluid injection well Northstar 1. Twenty-one accurately located earthquakes are distributed along the pair of en echelon faults striking 265° (ENE-WSW) and dipping steeply to the north (dip = 72°N), consistent with the main shock focal mechanism.

[43] All the well-located earthquakes have occurred at depths ranging from 3.5 to 4.0 km in the Precambrian crystalline basement. Most of the previously known earthquakes associated with the fluid injections in the eastern United States have occurred in Precambrian basement indicating that tectonic strain stored in the crystalline basement is released through the triggered events (e.g., Ashtabula, Ohio [*Seeber et al*., 2004], and Guy, Arkansas [*Horton*, 2012]). The *P* axis of the main shock mechanism trends

NE-SW and corresponds to horizontal compression ($\sigma_{Hmax}$) which is slightly rotated from the ENE-WSW trending broad-scale regional stress field in the northeastern United States [*Du et al*., 2003; *Zoback and Zoback*, 1991].

[44] The first detected earthquake ($M_w$ 1.2) occurred on 11 January 2011, 13 days after the commencement of injection at Northstar 1 well. At that time, a total of ~700 $m^3$ of fluid had been injected at a rate of up to 5 $m^3$/h, and the surface injection pressure was up to 13.5 MPa. Total injection volume was a very small quantity when it started to trigger an earthquake, and the injection pressure was relatively low, and hence, there must have been nearly direct fluid conduits to the ENE-WSW trending fault very close to the injection wellbore, and the subsurface condition at the Precambrian basement may have been near critical for the earthquakes to occur. The cross correlation between the earthquake series and the injection flow rate series indicates that the peak of seismicity follows the peak pressure with approximately five days lag. This short-term response of the injection media at Youngstown is similar to an observation at RMA where about 10 days of time lag in earthquake occurrences was observed following fluid injection [*Healy et al*., 1968].

[45] We conclude that the recent, 2011–2012, earthquakes in Youngstown, Ohio were induced by the fluid injection at Northstar 1 deep injection well due to increased pore pressure along the preexisting (ENE-WSW trending) faults located close to the wellbore in the Precambrian basement. This is based on the facts that: (1) well-located earthquakes clustered in a narrow zone along the fault trace striking ENE-WSW in the Precambrian basement (Figures 3 and 6); (2) migration of seismicity from the east—close to the injection point, toward the west—away from the wellbore, indicating that the expanding high fluid pressure front increased the pore pressure along its ENE-WSW trending path and progressively triggered the earthquakes; (3) occurrence of earthquakes was generally correlated with the total daily injection volume and injection pressure, and a pair of peaks in the injection parameters appears to be correlated with the occurrence of earthquakes at the early stage of fluid injection when the subsurface hydraulic system started to build up pore pressure; (4) 75% of the minima in surface injection pressure (no pumping operations) appeared to correlate with quiescent intervals of seismicity, which may indicate that the earthquakes were caused by the pressure buildup in the fractured Precambrian basement and stopped when pressure dropped; and (5) a short-term response of the injection media to the fluid injection parameters on the time scale of hours to few days (5+) suggests that the site behaved as a fractured Precambrian reservoir as in the Rocky Mountain Arsenal, Colorado.

[46] **Acknowledgments.** John Armbruster at Lamont-Doherty Earth Observatory of Columbia University (LDEO) led fieldwork in Youngstown, Ohio and processed raw data during January–March 2012. Chris Grope at Youngstown State University participated in the fieldwork and helped in portable station service and data retrieval. Mike Hansen and Tim Leftwitch of the Ohio Division of Geological Survey, Ohio Department of Natural Resources, helped to carry out the fieldwork and supported this study, as well as provided well log data and other material for the study. Jeffrey Dick of Youngstown State University helped us to deploy a NetQuake station, YSLD, at the campus. Larry Smyers of D&L Energy Inc. provided a spreadsheet of injection parameters at Northstar 1 well. Paul Richards and Heather Savage at LDEO provided critical comments that improved the paper. Alberto Malinverno helped to interpret well logging data. I thank Bill Menke for helping me with Poisson distribution. Stephen Holtkamp and Michael Brudzinski of Miami University of Ohio shared their result of regional event detection which helped us to solidify detection of regional events down to $M_w$ ~0.5. Mitchell Gold of LDEO read the manuscript and provided editorial help. Bill Leith of U.S. Geological Survey supported the field work, and Bill Ellsworth and Art McGarr of USGS provided useful comments. The U.S. Geological Survey has provided partial support for this study under contract G10AC00094. This is Lamont-Doherty Earth Observatory contribution 7681 .

## References

Ake, J., K. Mahrer, D. O'Connell, and L. Block (2005), Deep-injection and closely monitored induced seismicity at Paradox Valley, Colorado, *Bull. Seismol. Soc. Am.*, *95*, 664–683.

Baranoski, M. T. (2002), Structure contour map on the Precambrian unconformity surface in Ohio and related basement features, report, *Div. Geol. Surv. Map PG-23,* scale 1:500,000, Ohio Dep. of Nat.l Resour., Columbus. [Available at http://www.dnr.state.oh.us/Portals/10/pdf/mappg23.pdf.]

Brown, W. A., C. A. Frohlich, W. L. Ellsworth, J. H. Luetgert, and M. R. Brunt (2012), The May 17th, 2012 M4.8 earthquake near Timpson, east Texas: Was it natural or was it induced?, Abstract S53I-06 presented at 2012 Fall Meeting, AGU, San Francisco, Calif., 3–7 Dec.

Brune, J. N. (1970), Tectonic stress and the spectra of seismic shear waves from earthquakes, *J. Geophys. Res.*, *75*, 4997–5009.

Brunt, M. R., W. A. Brown, and C. A. Frohlich (2012), Felt reports and intensity maps for two M4.8 Texas earthquakes: 17 May 2012 near Timpson and 20 October 2011 near Fashing, Abstract S51E-2454 presented at 2012 Fall Meeting, AGU, San Francisco, Calif., 3–7 Dec.

Byerlee, J. D. (1978), Friction of rocks, *Pure Appl. Geophys.*, *116*, 615–626.

Davis, S. D., and W. D. Pennington (1989), Induced seismic deformation in the Cogdell oil field of west Texas, *Bull. Seismol. Soc. Am.*, *79*, 1477–1495.

Du, W.-X., W.-Y. Kim, and L. R. Sykes (2003), Earthquake source parameters and state of stress for northeastern United States and southeastern Canada from analysis of regional seismograms, *Bull. Seismol. Soc. Am.*, *93*, 1633–1648.

Ellsworth, W. L., S. H. Hickman, A. L. Llenos, A. McGarr, A. J. Michael, and J. L. Rubinstein (2012), Are seismicity rate changes in the midcontinent natural or manmade?, paper presented at 2012 Seismological Society of America Annual Meeting, San Diego, Calif.

Frohlich, C., C. Hayward, B. Stump, and E. Potter (2011), The Dallas-Fort Worth earthquake sequence: October 2008 through May 2009, *Bull. Seismol. Soc. Am.*, *101*, 327–340.

Gibbons, S. J., and F. Ringdal (2012), Seismic monitoring of the North Korea nuclear test site using a multichannel correlation detector, *IEEE Trans. Geosci. Remote Sens.*, *50*, 1897–1909, doi:10.1109/TGRS.2011.2170429.

Gibbs, J. F., J. H. Healy, C. B. Raleigh, and J. Coakley (1973), Seismicity in the Rangely, Colorado, area: 1962–1970, *Bull. Seismol. Soc. Am.*, *63*, 1557–1570.

Gomberg, J. S., K. M. Shedlock, and S. W. Roecker (1990), The effect of S-wave arrival times on the accuracy of hypocenter estimation, *Bull. Seismol. Soc. Am.*, *80*, 1605–1628.

Hansen, M. C. (2012), Earthquakes in Ohio, *Educ. Leaflet 9*, Div. of Geol. Surv., Ohio Dep. of Nat. Resour., Columbus. [Available at http://www.dnr.state.oh.us/Portals/10/pdf/EL/el09.pdf.]

Hansen, M. C., and L. J. Ruff (2003), The Ohio seismic network, *Seismol. Res. Lett.*, *74*, 561–564.

Healy, J. T., W. W. Rubey, D. T. Griggs, and C. B. Raleigh (1968), The Denver earthquakes, *Science*, *161*, 1301–1310.

Herrmann, R. B., S.-K. Park, and C.-Y. Wang (1981), The Denver earthquakes of 1967–1968, *Bull. Seismol. Soc. Am.*, *71*, 731–745.

Horton, S. (2012), Disposal of hydrofracking waste fluid by injection into subsurface aquifers triggers earthquake swarm in central Arkansas with potential for damaging earthquake, *Seismol. Res. Lett.*, *83*, 250–260, doi:10.1785/gssrl.83.2.250.

Hsieh, P. A., and J. S. Bredehoeft (1981), A reservoir analysis of the Denver earthquakes—A case study of induced seismicity, *J. Geophys. Res.*, *86*, 903–920.

Hubbert, M. K., and W. W. Rubey (1959), Role of fluid pressure in mechanics of overthrust faulting, *Geol. Soc. Am. Bull.*, *70*, 115–206.

Keranen, K., H. M. Savage, G. Abers, and E. S. Cochran (2013), Potentially induced earthquakes in Oklahoma, USA: Links between wastewater injection and the 2011 $M_W$ 5.7 earthquake sequence, *Geology*, *41*, 699–702, doi:10.1130/G34045.1.

Kim, W.-Y., and M. Chapman (2005), The 9 December 2003 central Virginia earthquake sequence: A compound earthquake in the central Virginia seismic zone, *Bull. Seismol. Soc. Am.*, *95*, 2428–2445.

Klein, F. W. (2007), User's guide to HYPOINVERSE-2000, a Fortran program to solve for earthquake locations and magnitudes, *U.S. Geol. Surv. Open File Rep., 02-171*, 121 pp.

Madariaga, R. (1976), Dynamics of an expanding circular fault, *Bull. Seismol. Soc. Am.*, *66*, 639–666.

McGarr, A. (1976), Seismic moments and volume changes, *J. Geophys. Res.*, *81*, 1487–1494.

McGarr, A. (2012), Factors influencing the seismic hazard of earthquakes induced by fluid injection at depth, paper presented at SPE/SEG Workshop on Injection Induced Seismicity, Soc. of Pet. Eng., Broomfield, Colo, 12–14 Sept. 2012.

McGarr, A., D. Simpson, and L. Seeber (2002), Case histories of induced and triggered seismicity, in *International Handbook of Earthquake and Engineering Seismology*, edited by W. Lee, H. Kanamori, P. Jennings, and C. Kisslinger, chap. 40, pp. 647–664, Academic Press, London.

Meremonte, M. E., J. C. Lahr, A. D. Frankel, J. W. Dewey, A. J. Crone, D. E. Overturf, D. L. Carver, and W. T. Bice (2002), Investigation of an earthquake swarm near Trinidad, Colorado, August–October 2001, *U.S. Geol. Surv. Open File Rep., 02-0073*.

National Academy of Sciences (2012), *Induced Seismicity Potential in Energy Technologies,* 225 pp., Natl. Acad. Press, Washington, D. C.

Nicholson, C., and R. L. Wesson (1992), Triggered earthquakes and deep well activities, *Pure Appl. Geophys.*, *139*, 561–578.

Nicholson, C., E. Roeloffs, and R. L. Wesson (1988), The northeastern Ohio earthquake of 31 January 1986: Was it induced?, *Bull. Seismol. Soc. Am.*, *78*, 188–217.

Ohio Department of Natural Resources (ODNR) (2012), Preliminary report on the Northstar 1 class II injection well and the seismic events in the Youngstown, Ohio, area, report, 23 pp., Columbus, March.

Raleigh, C. B., J. H. Healy, and J. D. Bredehoeft (1976), An experiment in earthquake control at Rangely, Colorado, *Science*, *91*, 1230–1237.

Rubinstein, J. L., W. L. Ellsworth, and A. McGarr (2012), The 2001–present triggered seismicity sequence in the Raton Basin of southern Colorado/northern New Mexico, Abstract S34A-02 presented at 2012 Fall Meeting, AGU, San Francisco, Calif., 3–7 Dec.

Schaff, D. P. (2008), Semiempirical statistics of correlation-detector performance, *Bull. Seismol. Soc. Am.*, *98*, 1495–1507.

Schaff, D. P., and F. Waldhauser (2010), One magnitude unit reduction in detection threshold by cross correlation applied to Parkfield (California) and China seismicity, *Bull. Seismol. Soc. Am.*, *100*, 3224–3238, doi:10.1785/0120100042.

Seeber, L., and J. G. Armbruster (1993), Natural and induced seismicity in the Erie-Ontario region: Reactivation of ancient faults with little neotectonic displacement, *Geogr. Phys. Quat.*, *47*, 363–378.

Seeber, L., J. Armbruster, and W. Y. Kim (2004), A fluid-injection-triggered earthquake sequence in Ashtabula, Ohio: Implications for seismogenesis in stable continental regions, *Bull. Seismol. Soc. Am.*, *94*, 76–87.

Shi, J., P. G. Richards, and W. Y. Kim (2000), Determination of seismic energy from *Lg* waves, *Bull. Seismol. Soc. Am.*, *90*, 483–493.

Stover, C. W., and Coffman, J. L. (1993), Seismicity of the United States, 1568–1989 (Revised), *U.S. Geol. Surv. Prof. Pap., 1527*, 418 pp.

Tadokoro, K., M. Ando, and K. Nishigami (2000), Induced earthquakes accompanying the water injection experiment at the Nojima fault zone, Japan: Seismicity and its migration, *J. Geophys. Res.*, *105*(B3), 6089–6104, doi:10.1029/1999JB900416.

Tadokoro, K., M. Ando, and K. Nishigami (2005), Correction to "Induced earthquakes accompanying the water injection experiment at the Nojima fault zone, Japan: Seismicity and its migration," *J. Geophys. Res.*, *110*, B03305, doi:10.1029/2004JB003602.

Viegas, G., K. Buckingham, A. Baig, and T. Urbancic (2012), Large scale seismicity related to wastewater injection near Trinidad, Colorado, USA, paper presented at GeoConvention 2012, Can. Soc. of Pet. Eng., Calgary, Alberta, Canada.

Waldhauser, F., and W. L. Ellsworth (2000), A double-difference earthquake location algorithm: Method and application to the northern Hayward fault, California, *Bull. Seismol. Soc. Am.*, *90*, 1353–1368.

Yeats, R. S., K. Sieh, and C. R. Allen (1997), *Geology of Earthquakes*, 568 pp., Oxford Univ. Press, New York.

Zhao, L. S., and D. V. Helmberger (1994), Source estimation from broadband regional seismograms, *Bull. Seismol. Soc. Am.*, *84*, 91–104.

Zoback, M. D., and H.-P. Harjes (1997), Injection-induced earthquakes and crustal stress at 9 km depth at the KTB deep drilling site, Germany, *J. Geophys. Res.*, *102*, 18,477–18,491.

Zoback, M. D., and J. H. Healy (1984), In situ stress measurements to 3.5 km depth in the Cajon Pass scientific research borehole: Implications for the mechanics of crustal faulting, *J. Geophys. Res.*, *97*, 5039–5057.

Zoback, M. D., and J. Townend (2001), Implications of hydrostatic pore pressures and high crustal strength for the deformation of intraplate lithosphere, *Tectonophysics*, *336*, 19–30.

Zoback, M. D., and M. L. Zoback (1991), Tectonic stress field of North America and relative plate motions, in *Neotectonics of North America*, edited by Slemmons et al. pp. 339–366, Geol. Soc. of Am., Boulder, Colo.

Zoback, M. L. (1992), Stress field constraints on intra-plate seismicity in eastern North America, *J. Geophys. Res.*, *97*, 11,761–11,782.